Transient Planetary Waves Simulated by GFDL Spectral General Circulation Models. Part I: Effects of Mountains

Y. HAYASHI AND D. G. GOLDER

Geophysical Fluid Dynamics Laboratory/NOAA, Princeton University, Princeton, NJ 08540

(Manuscript received 20 April 1982, in final form 12 November 1982)

ABSTRACT

Space-time spectral analysis over a three year data set is made of transient planetary waves simulated by Geophysical Fluid Dynamics Laboratory (GFDL) spectral general circulation models with and without mountains.

In both models westward moving ultralong waves have larger geopotential amplitude than eastward moving ultralong waves, being in agreement with observations. In both models westward moving ultralong waves are associated with little vertical tilt and a large meridional wavelength, while eastward moving ultralong waves are associated with some vertical tilt and a small meridional wavelength.

In the absence of mountains westward moving ultralong waves are somewhat decreased, while eastward moving ultralong waves are somewhat increased, and eastward moving wavenumber 4–6 components are markedly increased in the Northern Hemisphere.

1. Introduction

Observed transient planetary waves consist of both westward and eastward moving components. The westward moving components (wavenumber 1–2 and periods 5–15 days) are characterized by little vertical tilt. They attain their maximum and minimum pressure amplitudes in the midlatitudes and tropics, respectively. These waves are interpreted as external Rossby waves (see reviews by Madden, 1979; Walterscheid, 1980).

Although transient ultralong waves have a much smaller amplitude than stationary ultralong waves, it is important in weather forecasting to predict transient ultralong waves correctly, since they account for the intermittent amplification and phase shift of quasi-stationary waves. External Rossby waves can also be erroneously excited as free waves by a numerical prediction model if the initial data are not consistent with the model (Nakamura, 1976; Kirkwood and Derome, 1977; Lambert and Merilees, 1978). These waves have been identified as a source of error in some numerical prediction models (Daley *et al.*, 1981).

Geisler and Dickinson (1975, 1976), Schoeberl and Clark (1980), and Salby (1981) studied the structure of resonant external Rossby waves in a realistic basic state that were forced by an oscillating vertical velocity imposed at the lower boundary. They found fairly good agreement with the observed structure.

Although these external waves can exist as free waves, there must be some excitation mechanism to maintain them against the effects of dissipation. These external waves may be resonantly forced by the fluctuating zonal flow over mountains as studied by Garcia and Geisler (1981). These waves may be amplified by the instability of the multiple equilibrium states in which waves interact with the zonal mean in the presence of topography or zonally asymmetric thermal forcing as studied by Charney and Straus (1980) and Reinhold and Pierrehumbert (1982). These waves may also be maintained, even in the absence of topography, by the wave–wave interaction between unstable baroclinic waves and neutral external waves as studied by Loesch (1974).

On the other hand, the observed eastward moving ultralong waves (wavenumbers 1–3 and periods 10–30 days) are associated with some vertical tilt in contrast to westward moving waves (Pratt and Wallace, 1976; Sato, 1977; Böttger and Fraedrich, 1980; Mechoso and Hartmann, 1982). In the troposphere they have a smaller pressure amplitude, but a larger temperature amplitude than westward moving ultralong waves. These baroclinic ultralong waves may be forced by a fluctuating zonal flow over mountains (Hirota, 1971; Garcia and Geisler, 1981). They may also be amplified due to the topographic instability of the multiple equilibrium states (Charney and Straus, 1980). They may be, to some extent, maintained by the baroclinic instability of realistic zonal mean states studied by Hartmann (1979) who found that eastward moving ultralong waves with a narrow meridional width are associated with greater baroclinic instability than those with a wide meridional width which were studied by Green (1960).

In view of the above observational and theoretical

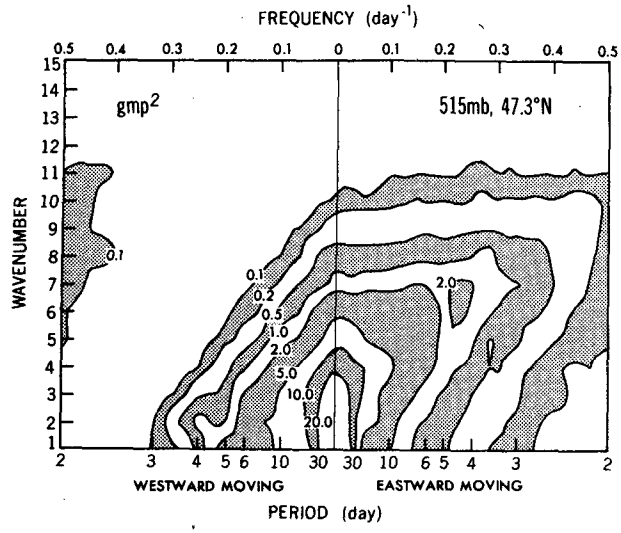

FIG. 1. Wavenumber–frequency distribution of the space–time power spectra (m^2) per unit frequency interval (1/365 day^{-1}) of geopotential height at 515 mb, 47.3°N over three years simulated by the model with mountains. The westward moving components with periods shorter than three days are aliased from the eastward moving components with periods shorter than two days.

background, it is of interest to examine the effect of mountains on the maintenance of transient planetary waves by use of a general circulation model. Manabe and Terpstra (1974) found that simulated transient eddy kinetic energy, as a whole, was markedly increased by eliminating mountains from their 9-level general circulation model, whereas stationary eddy kinetic energy was markedly decreased. Hayashi and Golder (1977) made a space–time spectral analysis of planetary waves in the Northern Hemisphere simulated by an 11-level GFDL grid point model. They found that westward moving waves were weaker than eastward moving waves, contrary to those observed. This defect was also found in other models such as an NCAR model (Pratt, 1979), and a GLAS model (Straus and Shukla, 1981). However, this defect seems to be alleviated in a current GFDL spectral model, according to a preliminary space–time spectral analysis (Hayashi, 1981).

In Part I of the present paper, a space–time spectral analysis is made of current GFDL spectral models with and without mountains to examine the possible effects of mountains on the maintenance of westward and eastward moving planetary waves. In Section 2, brief descriptions of the models are given. In Section 3 a space–time spectral analysis of the model data is presented. Conclusions and remarks are given in Section 4.

In Part II (Hayashi and Golder 1983), the energetics of the simulated transient planetary waves are analyzed to study how these waves are maintained.

2. Brief descriptions of models

The present analysis compares 9-level, 15-wavenumber (rhomboidal truncation) spectral general cir-

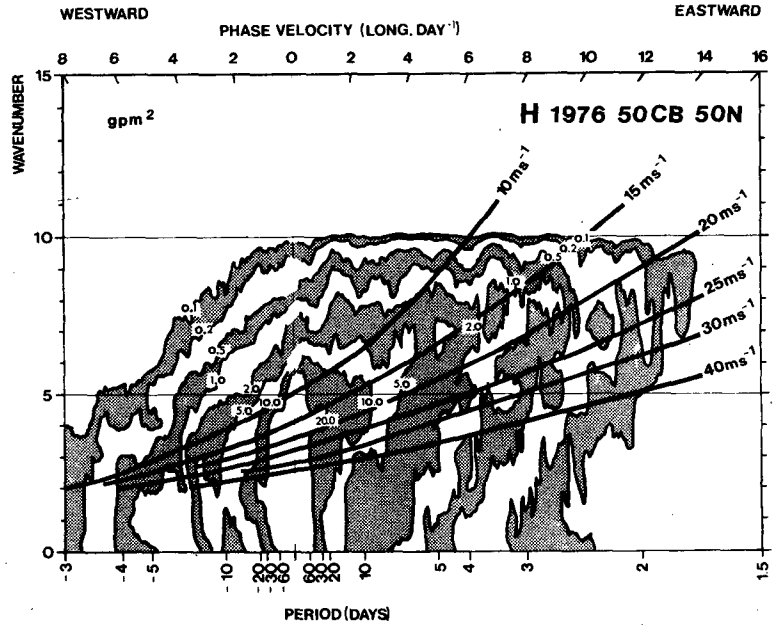

FIG. 2. Wavenumber–frequency distribution of the observed space–time power spectra (m^2) per unit frequency interval (1/365 day^{-1}) of geopotential height at 500 mb, 50°N over one year (after Speth and Kirk, 1981). The solid lines represent the dispersion relations of nondivergent Rossby waves ($C = U - \beta/k^2$) for different mean flows.

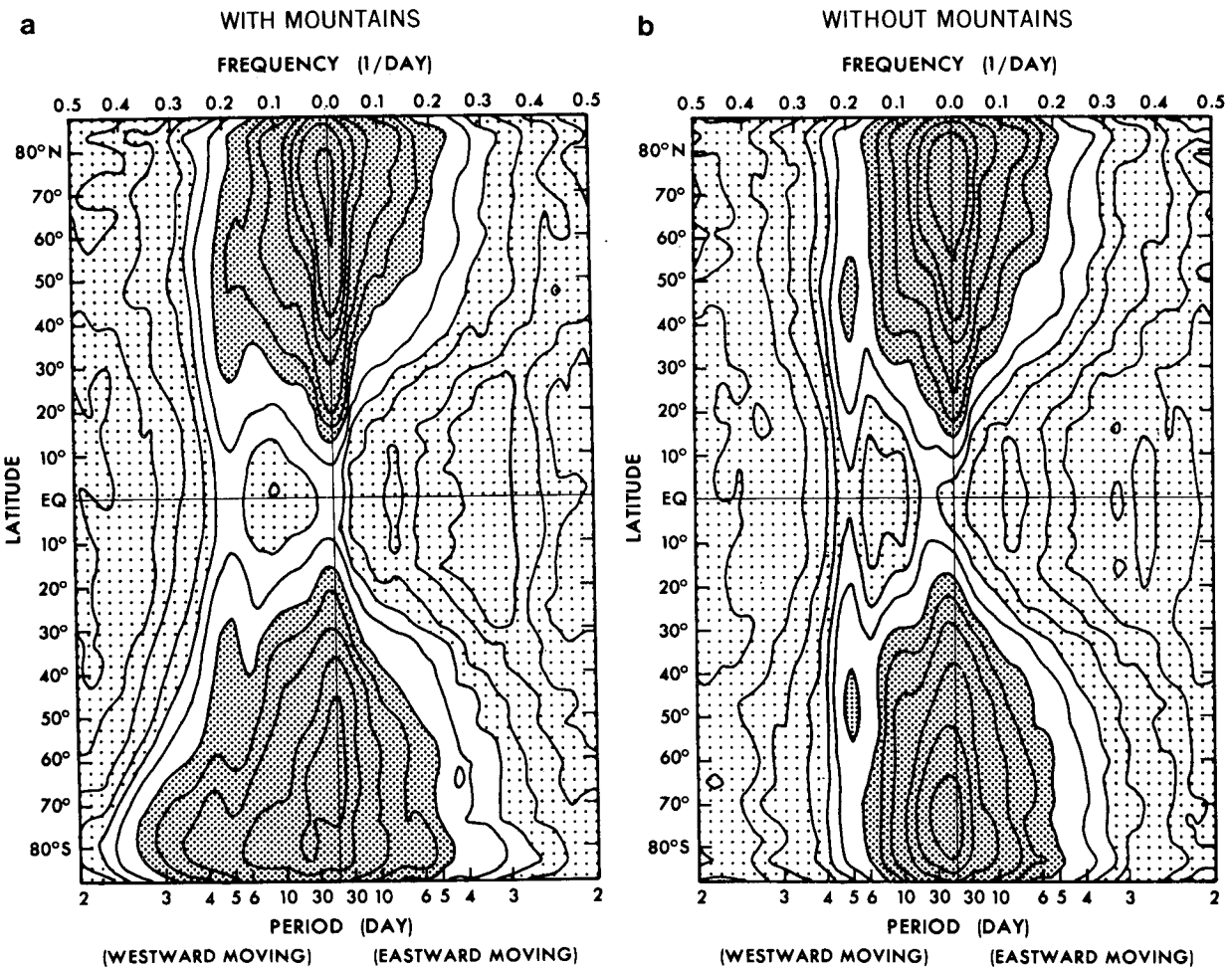

FIG. 3. Latitude–frequency distribution (wavenumber 1) of the space–time power spectral density (m^2 day) of geopotential height at 515 mb over three years (a) with, and (b) without mountains. Dark shade indicates greater than 500, light shade less than 100. Contour intervals 10, 20, 50, 100, 200, 500, 1000, 2000, 5000, 10 000. These values should be divided by 365 to be consistent with the units in Figs. 1 and 2.

culation models (Manabe *et al.*, 1979) with and without mountains. The effect of mountains is incorporated by use of the so-called "sigma coordinate system." The imposed insolation and sea surface temperature undergo seasonal but no interannual or diurnal variations. Temperatures of the land surfaces are determined in such a way that they satisfy a heat balance. The effect of moist convection is represented by the moist convective adjustment. A detailed description of the GFDL spectral models is given by Gordon and Stern (1982).

3. Space–time spectral analysis

The space–time cross spectra were estimated through the time cross-spectra of the zonal Fourier coefficients by use of the formulas derived by Hayashi (1971). The method and applications of space–time spectral analysis are reviewed in Hayashi (1982). In order to give sufficient statistical significance, the analysis was performed over the three year period (including all the seasons) of each model by use of daily time series sampled from model years 13–15 (with mountains) and 10–12 (without mountains). The time cross-spectra were computed by the lag correlation method with a 30-day Tukey lag window. The frequency resolution is 1/60 day^{-1} and the number of degrees of freedom is 97.

a. Spectral distributions

Fig. 1 shows the wavenumber–frequency distribution of the space–time power spectra of geopotential height at 515 mb, 47.3°N simulated by the model with mountains. In particular, it should be noted that for periods shorter than 30 days, the westward moving component of low wavenumbers is stronger than the eastward moving component, in agreement with the

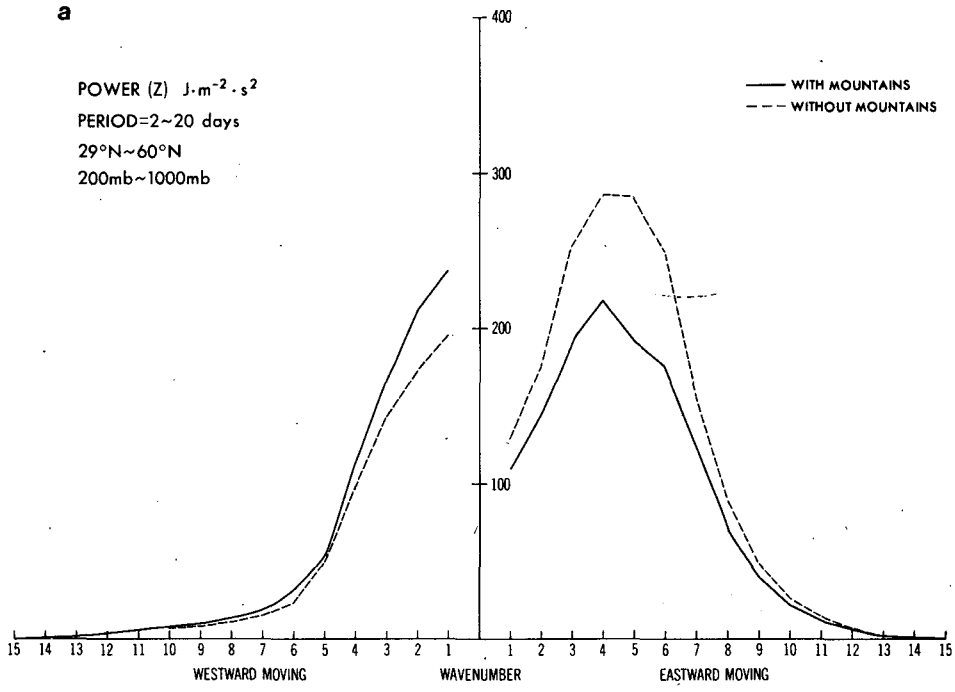

FIG. 4. Space–time power spectra of geopotential height integrated over periods of (a) 2–20 days; (b) 2–7 days; (c) 7–20 days, for 29–60°N and 200–1000 mb with (solid) and without (dashed) mountains.

observed spectra at 50°N (Speth and Kirk, 1981) over one year shown in Fig. 2. This agreement indicates an improvement of this spectral model over an 11-level GFDL grid model analyzed by Hayashi and Golder (1977) and Pratt (1979), who found that the westward moving component is weaker than the eastward moving component contrary to those observed.

Fig. 3 compares the latitude–frequency distribution (wavenumber 1) of the space–time spectral density of geopotential height at 515 mb, simulated by the model with and without mountains. A spectral peak corresponding to the observed westward moving 5-day period waves[1] is more clearly seen in the model without mountains (Fig. 3b) than in the model with mountains (Fig. 3a), although the amplitude is somewhat smaller.

Fig. 4 shows the wavenumber distribution of the space–time power spectra (periods 2–20 days, 2–7 days, 7–20 days) of geopotential height integrated over 200–1000 mb and 29–60°N. It can be seen that in the absence of mountains, the power spectra of westward moving ultralong waves are somewhat decreased, while the eastward moving ultralong waves are somewhat increased. In particular, the eastward moving wavenumber 4–6 components are markedly increased. This result is consistent with that of Manabe and Terpstra (1974), who found that the simulated transient-eddy kinetic energy as a whole is markedly increased in the absence of mountains in the Northern Hemisphere. The effects of mountains on the general circulation of the Southern Hemisphere were studied by Mechoso (1981).

b. Wave structure

Fig. 5 shows the vertical structure of geopotential height with and without mountains at 47.3°N for wavenumber 1 and westward periods of 5 and 15 days. These periods are chosen to represent fast and slow moving waves. Both 5 and 15 day period waves in the two models increase in amplitude with height. They have no tilt in the troposphere as observed (e.g. Madden, 1978). Unlike the 15-day waves, the 5-day waves shows high coherence between stratosphere and troposphere. The coherence required to reject a null hypothesis of no coherence at the 95% confidence level is above 0.24 for 97 degrees of freedom (see Julian, 1975; Thompson, 1979).

The meridional structure of these westward moving waves at 515 mb is shown in Fig. 6. Both 5- and 15-day waves (Fig. 6a and b) in the two models attain their maximum and minimum amplitudes in the midlatitudes and tropics, respectively. They are nearly symmetric with respect to the equator. The large co-

[1] The observed 5-day period waves are based on winter time data. This spectral peak is not clearly seen in Fig. 2 (observed one year spectra), although this period is dominated by a westward moving component.

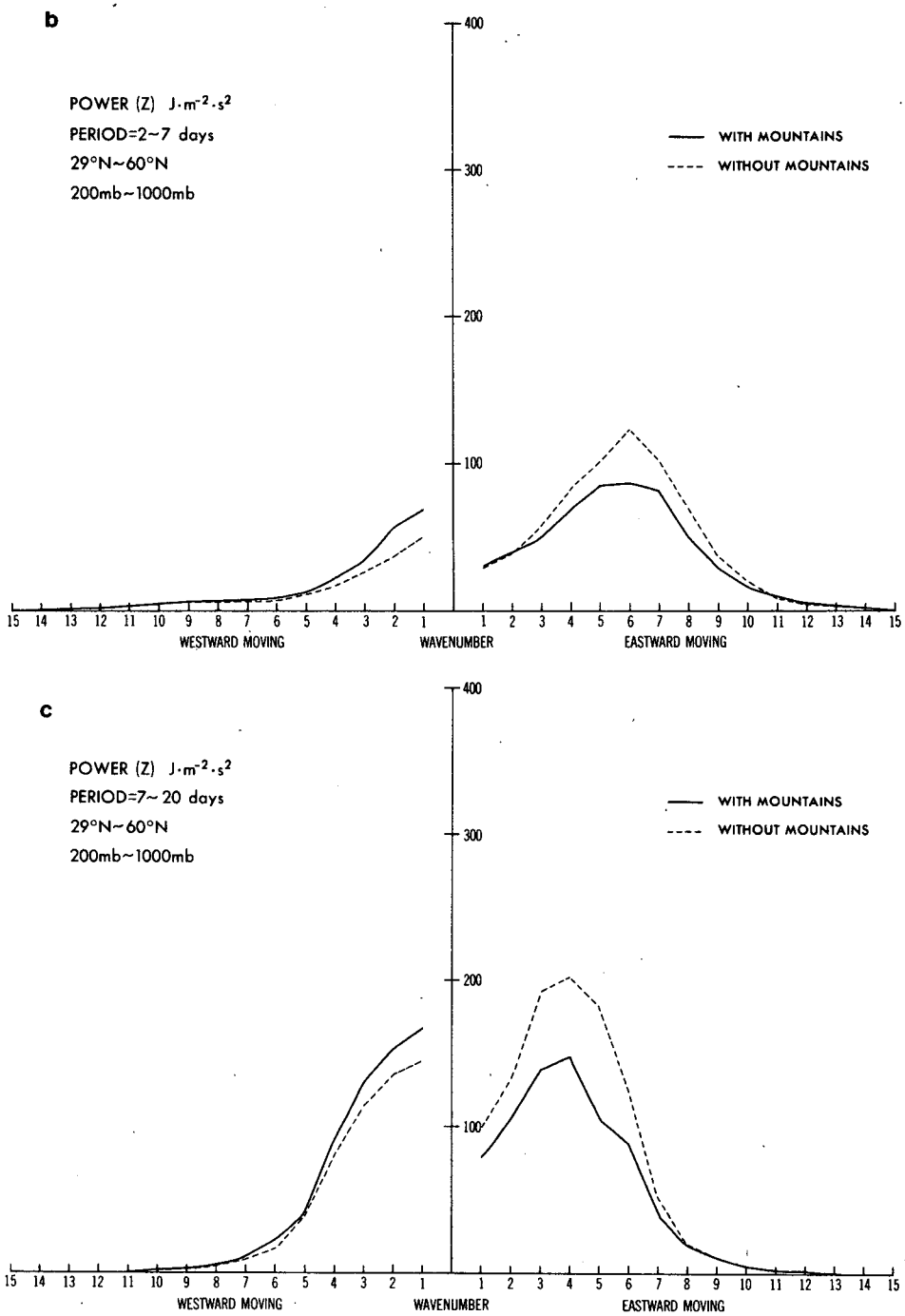

FIG. 4. (*Continued*)

herence and little phase change for the 5-day wave suggests a large meridional wavelength. Unlike the 5-day waves, the 15-day waves exhibit a 180° phase reversal near 30° latitudes. The latitudinal structure of the 5- and 15-day wave is identifiable with that of the nondivergent Rossby–Haurwitz wave over a sphere for $(m, n) = (1, 2)$ and $(1, 4)$ as illustrated by Fig. 7 (after Madden, 1979). Salby's (1981) calculations with a realistic equinox and solstice basic states suggest that this identification is basically correct in the troposphere.

The vertical structure of geopotential height at

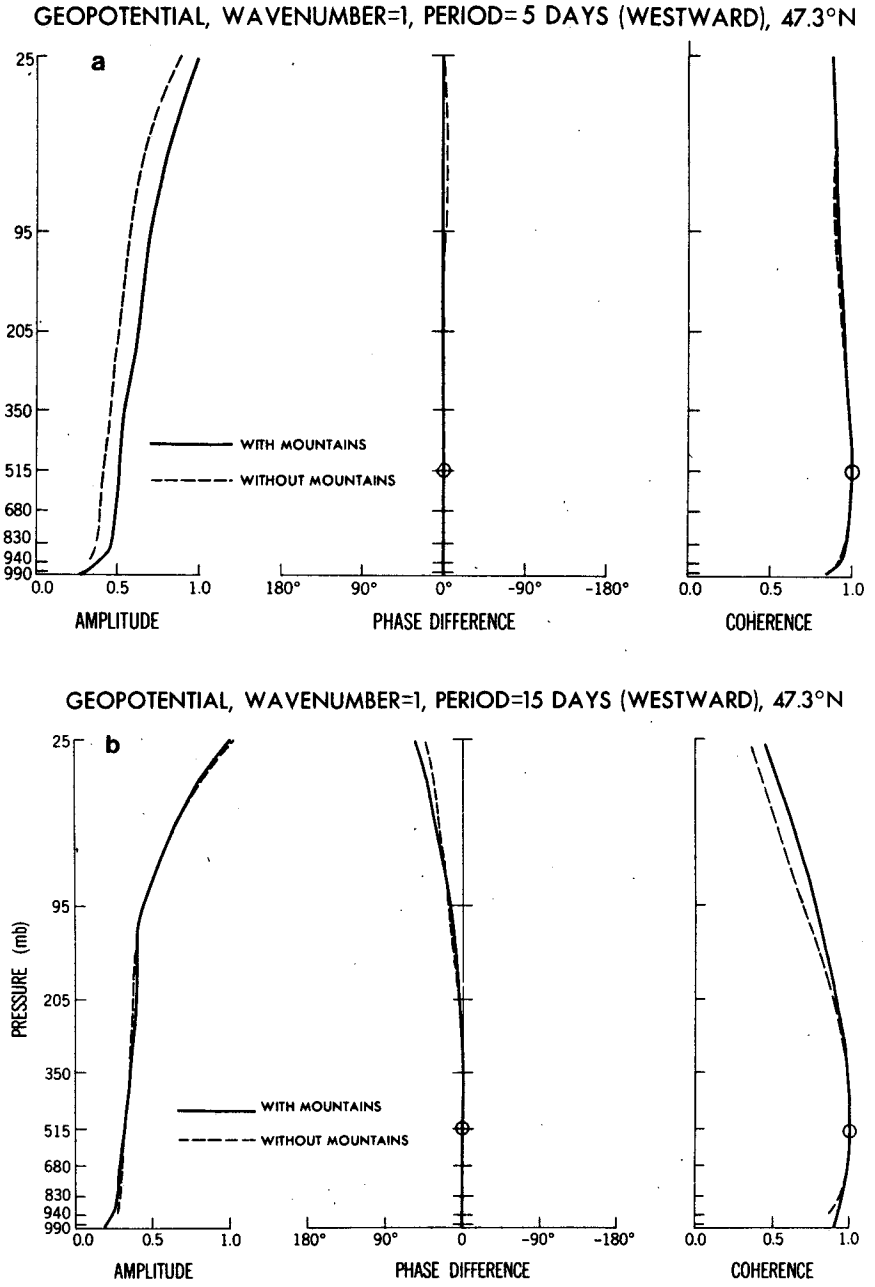

FIG. 5. Vertical structure of geopotential height (wavenumber 1) at 47.3°N for a westward period of (a) 5 days and (b) 15 days, with (solid) and without (dashed) mountains. The reference level (515 mb) of phase difference and coherence is indicated by open circles.

47.3°N for wavenumber 2 and eastward periods of 20 days is given in Fig. 8. In contrast to the westward moving components, this eastward moving component exhibits some phase variation in both the models in agreement with those observed (Pratt and Wallace, 1976; Sato, 1977; Böttger and Fraedrich, 1980).

The meridional structure of the eastward moving component (wavenumber 2 and period 20 days) at 515 mb is shown in Fig. 9. Since this mode has 180° phase reversals at 30 and 60° latitudes in both the models, its meridional wavelength is smaller than that of the westward moving components (Fig. 6).

4. Conclusions and remarks

On the basis of space–time spectral analysis over 3-year data from 9-layer GFDL spectral general circulation models with and without mountains, the following conclusions have been reached.

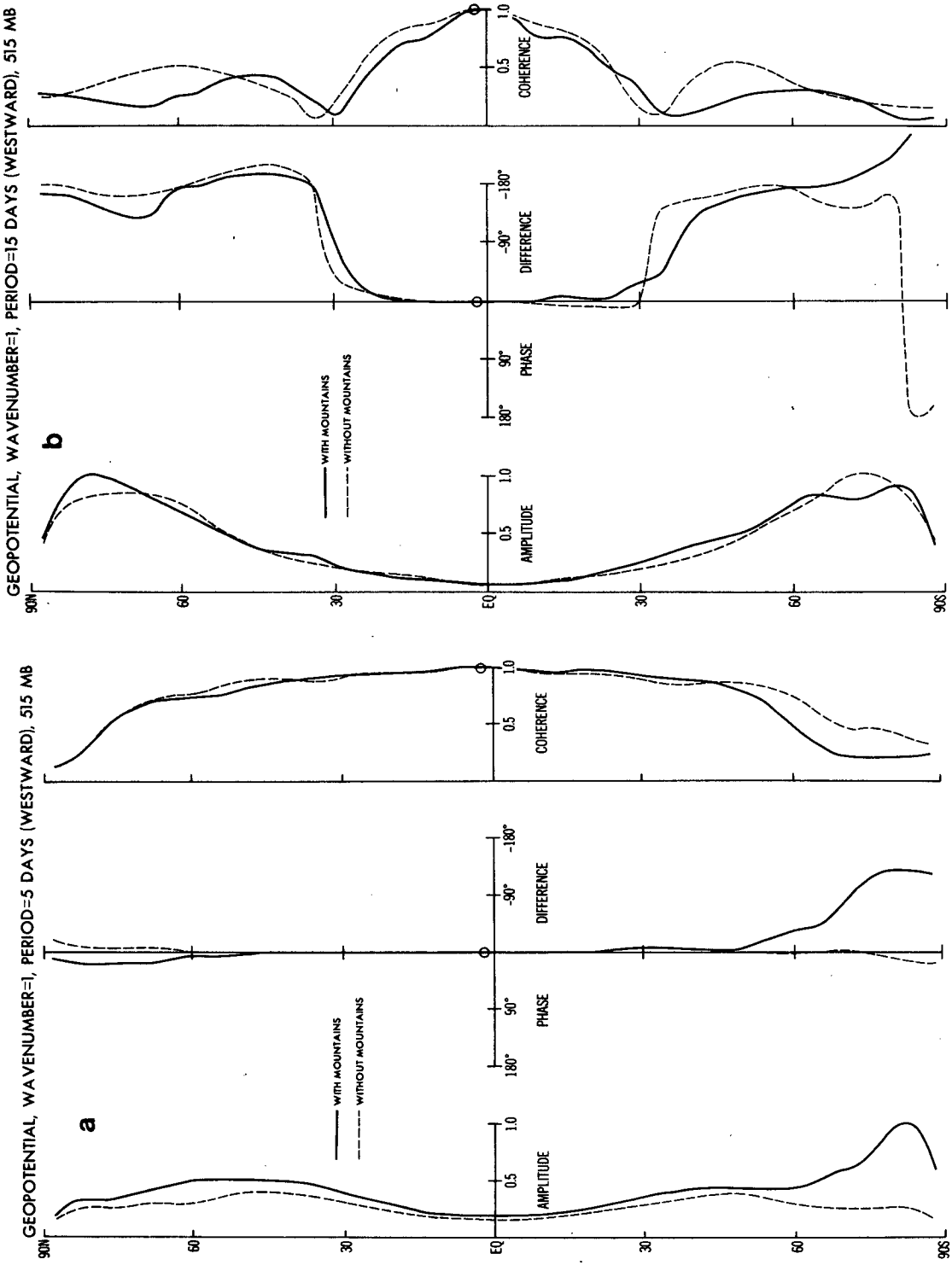

FIG. 6. Latitudinal structure of the geopotential height (wavenumber 1) at 515 mb for *westward* periods of (a) 5 days and (b) 15 days, with (solid) and without (dashed) mountains. The reference latitude (2.3°N) is indicated by open circles.

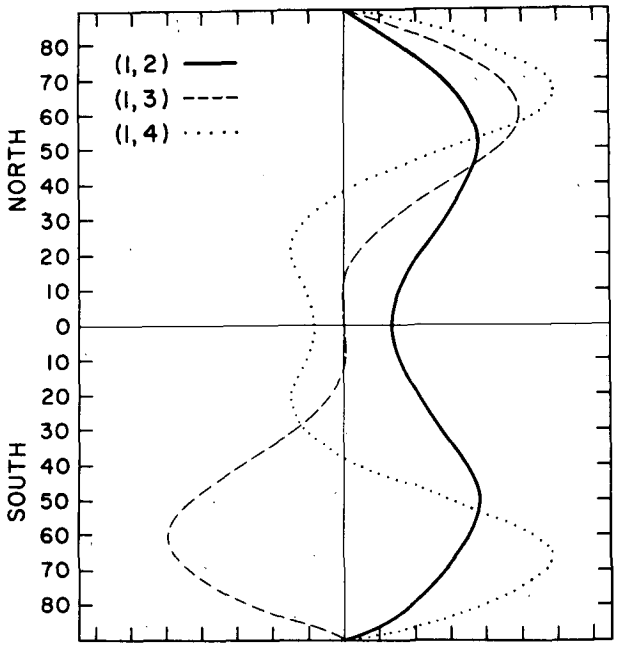

FIG. 7. Latitudinal structure of the geopotential height field of nondivergent Rossby–Haurwitz waves over a sphere for $m = 1$, $n = 2, 3, 4$ modes where m is the zonal wavenumber and $n-m$ is the meridional mode number (after Madden, 1979).

1) In both models the power spectra of geopotential height in the midlatitude troposphere is associated with more westward than eastward moving components for wavenumbers 1–2 and periods 5–20 days in agreement with observations in the Northern Hemisphere.

2) In both models, the westward moving components (wavenumber 1 and periods 5 and 15 days) are characterized by little vertical tilt, particularly in the troposphere, and large meridional wavelengths, while the eastward moving component (wavenumber 2 and period 20 days) is associated with some westward vertical tilt and small meridional wavelength.

3) In the absence of mountains, westward moving ultralong waves (periods 2–20 days) are somewhat reduced, while eastward moving ultralong waves (periods 2–20 days) are somewhat increased in the Northern Hemisphere.

4) In the absence of mountains, eastward moving wavenumber 4–6 components are markedly increased in the Northern Hemisphere.

It is encouraging that both westward and eastward moving planetary waves are simulated rather well in the current GFDL spectral model. This is an improvement over the previous 11-level grid model in which westward moving ultralong waves were weaker than eastward moving ultralong waves, contrary to observations. This improvement might be partly related to the fact that the present model has a more realistic zonal flow (see Manabe *et al.*, 1979) than the previous model which produces westerlies that are too strong in the stratosphere (see Hayashi and Golder, 1977).

It is of interest to note that mountains have different effects on the eastward and westward moving components. This suggests that mountains do not merely force standing wave oscillations but also affect traveling waves. It is also of importance that both

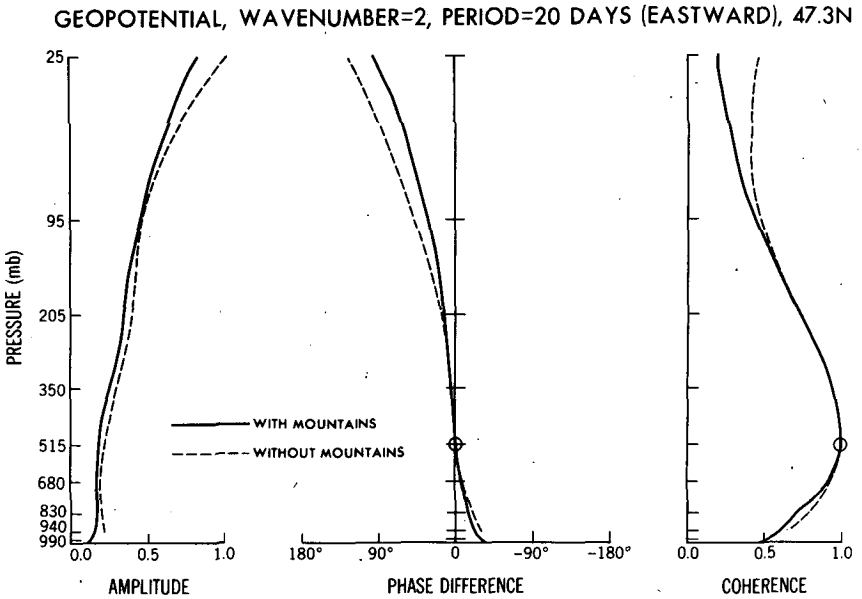

FIG. 8. Vertical structure of geopotential height (wavenumber 1) at 47.3°N for an eastward moving period of 20 days with (solid) and without (dashed) mountains. The reference level (515 mb) is indicated by open circles.

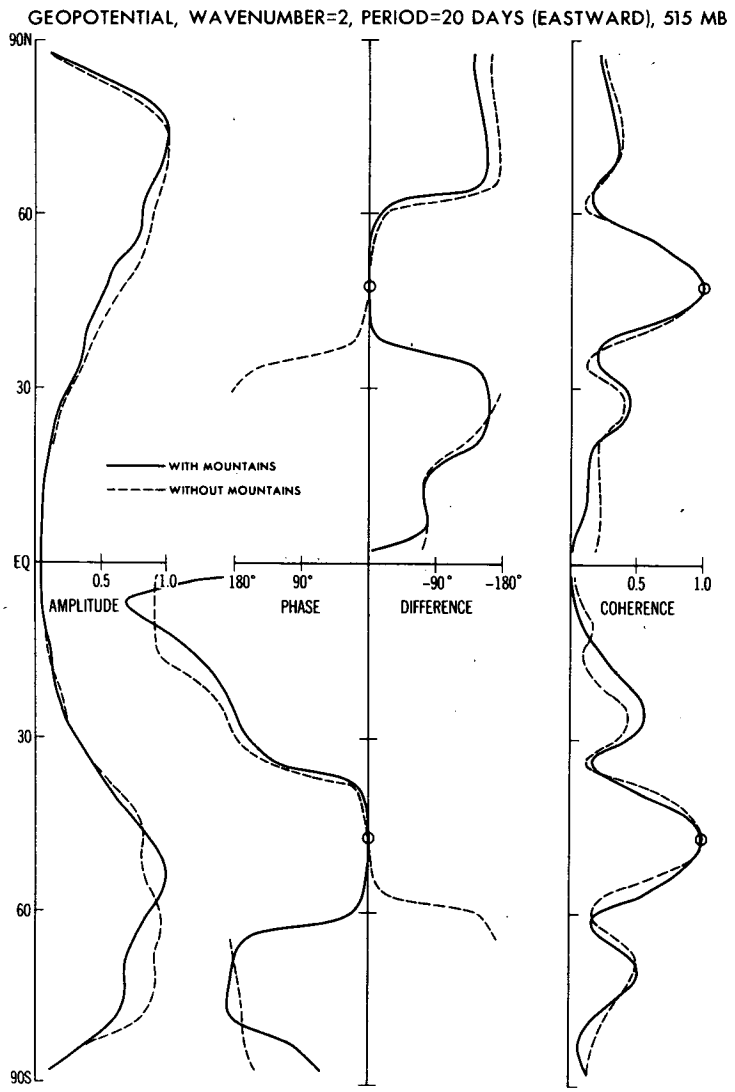

FIG. 9. Latitudinal structure of geopotential height (wavenumber 2) at 515 mb for *eastward* periods of 20 days with (solid) and without (dashed) mountains. The reference latitudes (47.3°N and 47.3°S) are indicated by open circles.

westward and eastward moving planetary waves do appear even in the absence of mountains. This suggests that mountains are not essential for the long-term maintenance of these waves, although they might have some indirect influence on the intermittent amplification of them.

In Part II, the energetics of simulated transient planetary waves are analyzed to study how these waves are maintained.

Acknowledgments. The authors wish to express their hearty gratitude to Dr. S. Manabe for his valuable advice and to Dr. J. Smagorinsky for his support of the research. Appropriate comments on the original manuscript from Dr. I. Held and Dr. G. P. Williams, and two anonymous reviewers, are greatly appreciated. Thanks are extended to Ms. J. Kennedy for typing, Mr. P. G. Tunison for drafting and Mr. J. N. Connor for photographing.

REFERENCES

Böttger, H., and K. Fraedrich, 1980: Disturbances in the wavenumber-frequency domain observed along 50°N. *Contrib. Atmos. Phys.*, **53**, 90–106.

Charney, J. G., and D. M. Straus, 1980: Form-drag instability, multiple equilibria and propagating planetary waves in baroclinic, orographically forced, planetary wave systems. *J. Atmos. Sci.*, **37**, 1157–1176.

Daley, R., J. Tribbia and D. L. Williamson, 1981: The excitation of large-scale free Rossby waves in numerical weather prediction. *Mon. Wea. Rev.*, **109**, 1836–1861.

Garcia, R. R., and J. E. Geisler, 1981: Stochastic forcing of small-

amplitude oscillations in the stratosphere. *J. Atmos. Sci.*, **38,** 2187–2197.

Geisler, J. E., and R. E. Dickinson, 1975: External Rossby modes on a β-plane with realistic vertical wind shear. *J. Atmos. Sci.*, **32,** 2082–2093.

——, and ——, 1976: The five day wave on a sphere with realistic zonal winds. *J. Atmos. Sci.*, **33,** 632–641.

Gordon, C. T., and W. F. Stern, 1982: A description of the GFDL global spectral model. *Mon. Wea. Rev.*, **110,** 625–644.

Green, J. S. A., 1960: A problem in baroclinic stability. *Quart. J. Roy. Meteor. Soc.*, **86,** 237–251.

Hartmann, D. L., 1979: Baroclinic instability of realistic zonal mean states to planetary waves. *J. Atmos. Sci.*, **36,** 2336–2349.

Hayashi, Y., 1971: A generalized method of resolving disturbances into progressive and retrogressive waves by space Fourier and time-cross spectral analyses. *J. Meteor. Soc. Japan,* **49,** 125–128.

——, 1981: Space-time cross spectral analysis using the maximum entropy method. *J. Meteor. Soc. Japan,* **59,** 620–624.

——, 1982: Space-time spectral analysis and its applications to atmospheric waves. *J. Meteor. Soc. Japan,* **60,** 156–171.

——, and D. G. Golder, 1977: Space-time spectral analysis of mid-latitude disturbances appearing in a GFDL general circulation model. *J. Atmos. Sci.*, **34,** 237–262.

——, and ——, 1983: Transient planetary waves simulated by GFDL spectral general circulation models. Part II: Effects of nonlinear energy transfer. *J. Atmos. Sci.*, **40,** 951–957.

Hirota, I., 1971: Excitation of planetary Rossby waves in the winter stratosphere by periodic forcing. *J. Meteor. Soc. Japan,* **49,** 439–449.

Julian, P. R., 1975: Comments on the determination of significance levels of the coherence statistics. *J. Atmos. Sci.*, **32,** 836–837.

Kirkwood, E., and J. F. Derome, 1977: Some effects of the upper boundary condition and vertical resolution on modeling forced stationary, planetary waves. *Mon. Wea. Rev.*, **105,** 1239–1312.

Lambert, S. J., and P. E. Merilees, 1978: A study of planetary wave errors in a spectral numerical weather prediction model. *Atmos. Ocean,* **16,** 197–211.

Loesch, A. Z., 1974: Resonant interactions between unstable and neutral baroclinic waves: Part I and Part II. *J. Atmos. Sci.*, **31,** 1177–1217.

Madden, R. A., 1978: Further evidence of traveling planetary waves. *J. Atmos. Sci.*, **35,** 1605–1618.

——, 1979: Observations of large-scale traveling Rossby waves. *Rev. Geophys. Space Phys.*, **17,** 1935–1949.

Manabe, S., and T. B. Terpstra, 1974: The effects of mountains on the general circulations of the atmosphere as identified by numerical experiments. *J. Atmos. Sci.*, **31,** 3–42.

——, D. G. Hahn and J. L. Holloway, Jr., 1979: Climate simulations with GFDL spectral models of the atmosphere: Effect of truncation. GARP Publ. Ser., No. 22, Vol. 1, 41–94.

Mechoso, C. R., 1981: Topographic influence on the general circulation of the Southern Hemisphere: A numerical experiment. *Mon. Wea. Rev.*, **109,** 2131–2139.

——, and D. L. Hartmann, 1982: An observational study of traveling planetary waves in the Southern Hemisphere. *J. Atmos. Sci.*, **39,** 1921–1935.

Nakamura, H., 1976: Some problems in reproducing planetary waves by numerical models of the atmosphere. *J. Meteor. Soc. Japan,* **54,** 129–146.

Pratt, R. W., and J. M. Wallace, 1976: Zonal propagation characteristics of large-scale fluctuations in the mid-latitude troposphere. *J. Atmos. Sci.*, **33,** 1184–1194.

——, 1979: A space-time spectral comparison of the NCAR and GFDL general circulation models to the atmosphere. *J. Atmos. Sci.*, **36,** 1681–1691.

Reinhold, B. B., and R. T. Pierrehumbert, 1982: Dynamics of weather regimes: Quasi-stationary waves and blocking. *Mon. Wea. Rev.*, **110,** 1105–1145.

Salby, M. L., 1981: Rossby normal modes in nonuniform background configurations. Part I: Simple fields. Part II: Equinox and solstice conditions. *J. Atmos. Sci.*, **38,** 1803–1840.

Sato, Y., 1977: Transient planetary waves in the winter stratosphere. *J. Meteor. Soc. Japan,* **55,** 89–106.

Schoeberl, M. R., and J. H. E. Clark, 1980: Resonant planetary waves in a spherical atmosphere. *J. Atmos. Sci.*, **37,** 20–28.

Speth, P., and E. Kirk, 1981: A one year study of power spectra in wavenumber–frequency domain. *Contrib. Atmos. Phys.*, **54,** 186–206.

Straus, D. M., and J. Shukla, 1981: Space-time spectral structure of a GLAS general circulation model and a comparison with observations. *J. Atmos. Sci.*, **38,** 902–917.

Thompson, R. O. R. Y., 1979: Coherence significance levels. *J. Atmos. Sci.*, **36,** 2020–2021.

Walterscheid, R. L., 1980: Traveling planetary waves in the stratosphere. *Pure Appl. Geophys.*, **118,** 239–265.